TEXTURE-ELICITED VIBRATIONS STRETCH OR CONTRACT SYSTEMATICALLY DEPENDING ON SCANNING SPEED

Charles M. Greenspon[1], Kristine R. McLellan[1], Justin D. Lieber[2], and Sliman J. Bensmaia[1,2]

1 - Department of Organismal Biology and Anatomy, University of Chicago, Chicago, IL

2 - Committee on Computational Neuroscience, University of Chicago, Chicago, IL

ABSTRACT

To sense the texture of a surface, we run our fingers across it, which leads to the elicitation of skin vibrations that depend both on the surface microgeometry and on exploratory parameters, particularly scanning speed. The transduction and processing of these vibrations mediates the ability to discern fine surface features. In the present study, we seek to characterize the effect of changes in scanning speed on texture-elicited vibrations to better understand how speed shapes the neuronal representation of texture. To this end, we scanned a variety of textures across the fingertip of human participants at a variety of speeds (10 – 160 mm/s) while measuring the resulting vibrations using a laser Doppler vibrometer. We found that increases in speed led to systematic increases in vibratory power and to a systematic upward shift in the frequency composition of the vibrations. Furthermore, we show that the increase in power can be explained by the upward shift in frequency composition. The enhancement of higher frequency components accounts for the observed increase in the firing rates of nerve fibers, particularly Pacinian corpuscle-associated fibers, which are most sensitive at the high frequencies.

INTRODUCTION

To discern the texture of a surface, we spontaneously run our fingers across it (1), an exploratory procedure that results in the elicitation of skin vibrations that reflect the microstructure of the surface. While coarse textural features can be sensed without movement, our perception of fine textural features relies on the processing of skin vibrations elicited during scanning (2–5). Two populations of tactile nerve fibers – rapidly adapting (RA) and Pacinian (PC) fibers – are exquisitely sensitive to skin vibrations and produce millisecond-precision temporal spiking sequences that reflect the vibrations (3,4,6,7). These vibration-sensitive afferents mediate our ability to perceive fine textural features as evidenced by the fact that desensitizing them results in impaired fine texture perception (5).

Texture-elicited vibrations are not only sensitive to surface microstructure but also to exploratory parameters, particularly scanning speed. Indeed, skin vibrations dilate or contract with decreases or increases in scanning speed (3,7), respectively, resulting in concomitant dilations or contractions of the evoked spiking sequences in the nerve (6). In addition, the firing rates of nerve fibers and of their downstream targets tend to increase with increases in scanning speed (8,9). Whether this enhanced neural response reflects the contraction of the spike trains or is caused by an increase in the intensity of the vibrations – which would also lead to higher firing rates – remains to be elucidated.

To fill this gap, we sought to systematically characterize how texture-evoked vibrations are shaped by scanning speed. To this end, we used a laser Doppler vibrometer to measure the vibrations evoked in the skin when everyday textures are scanned across the skin over a range of behaviorally relevant speeds (10). Previous measurements of the effect of speed on vibratory power were obtained with textures scanned at a single speed through each experimental block (7) and, given the measurement approach, the overall gain of the measurements varied from block to block. As a result, the raw magnitude of the vibrations could not be compared across experimental blocks and so the effect of speed on magnitude could not be assessed.

Across a wide range of scanning speeds, we find that (as expected) vibratory intensity increases with speed but does so in a texture-specific way. We then demonstrate that changes in vibratory intensity with scanning speed can be explained by the expected shift in the frequency composition of the vibrations. We discuss the implications of these findings for the neural coding of both texture and speed.

RESULTS

We used a custom-built rotating drum stimulator (**Figure 1a**) to scan 8 textured surfaces across the right index fingertip of 5 human subjects (2 male, 3 female, age range 20-25 years) while measuring the evoked skin vibrations using a laser Doppler vibrometer (Polytec OFV-3001 with OFV 311 sensor head; Polytec, Irvine, CA) (**Figure 1b**). The surfaces (**Figure 1c**) were scanned at 28 speeds (10 – 160 mm/s) to characterize how texture and scanning speed modify the vibrations (**Figure 1d**).

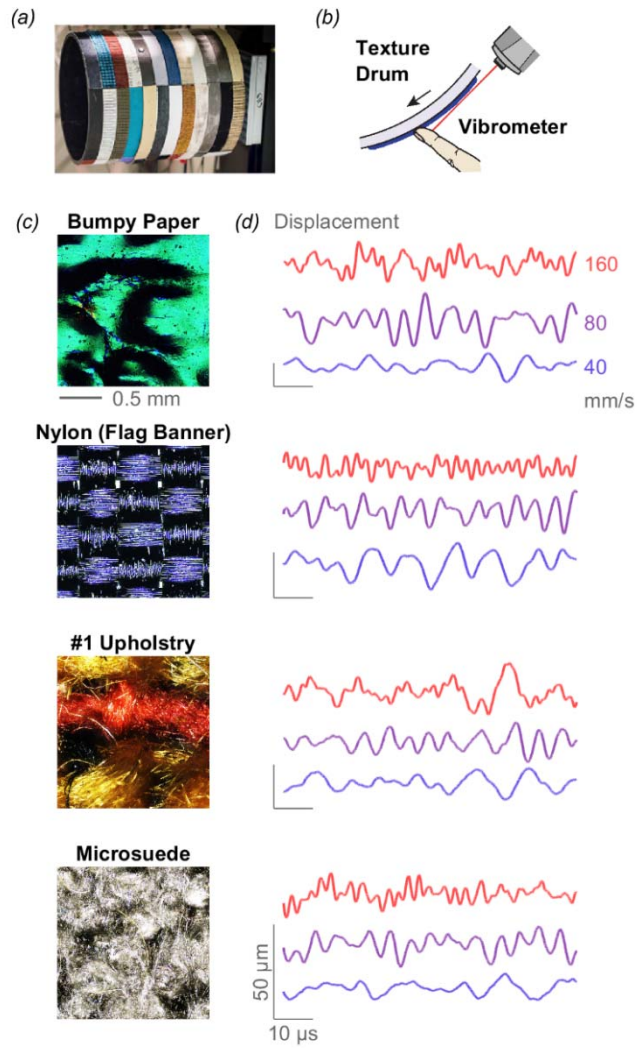

Figure 1 | Experimental setup and example vibrations. (*a*) The rotating drum stimulator used to scan textures across the fingertip. (*b*) Recording setup diagram showing finger, texture drum, and vibrometer. (*c*) High magnification photos of example textures along with vibrometry traces at three speeds (*d*). See **Supplementary Figure 1** for examples from all textures, along with RMS amplitude as a function of speed.

Effect of scanning speed on the intensity of texture-elicited vibrations

First, we found that the intensity of the vibrations elicited in the skin, as indexed by total vibratory energy, varied widely across textures ($F_{7,1118} = 430.62$, $p < 0.001$, $\eta^2 = 0.347$), as has been previously shown (7). Indeed, the energy varied over more than an order of magnitude at both the lowest (0.0255 to 23.3 mm2/s2) and highest speed (0.468 and 132 mm2/s2 at 160 mm/s). Second, we found that the energy increased concomitantly with the scanning speed (3-way ANOVA, $F_{27,1090} = 27.37$, $p < 0.001$, $\eta^2 = 0.099$) (**Figure 2a**) in a manner well approximated by linear regression ($R^2 = 0.766$). The effect of speed on energy was also texture-dependent, as evidenced by a significant texture x speed interaction ($F_{189,1090} = 2.78$, $p < 0.001$, $\eta^2 = 0.07$). Indeed, the energy increased between 2.5 to 120 times when comparing the lowest and highest speeds, depending on the texture. Vibratory energy did not just vary across textures but also across participants ($F_{3,1090} = 175.73$, $p < 0.001$, $\eta^2 = 0.07$) and the participant x speed interaction was weak but statistically significant ($F_{108,1090} = 1.73$, $p < 0.001$, $\eta^2 = 0.025$). Interestingly, though the absolute amount of energy clearly increased with speed, the magnitude of the skin displacement did not substantially change (**Supplementary Figure 1**). Thus, the observed energy increase with speed is driven by the rate at which the displacements occur and not their size.

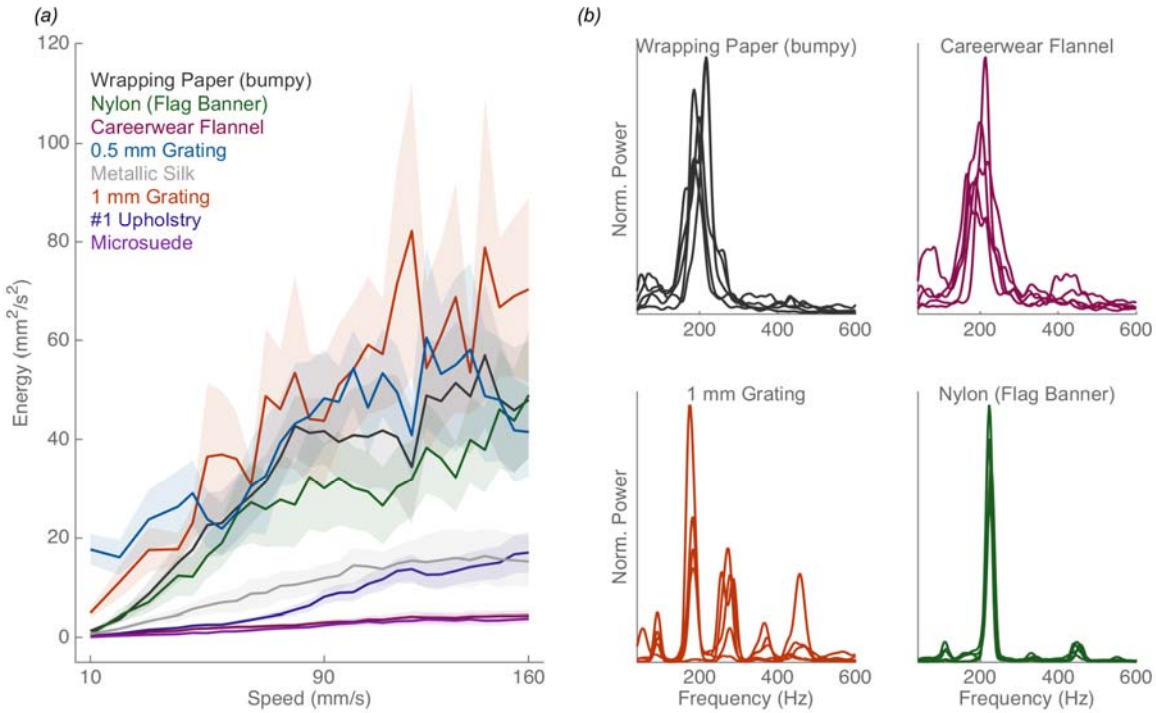

Figure 2 | The energy of texture-elicited vibrations increases as scanning speed increases. (*a*) Energy of the vibrations elicited by each texture vs. speed. (*b*) Normalized power spectral densities for four textures scanned at 80 mm/s for all participants. Power spectra for a given texture are similar across participants.

Effect of scanning speed on the frequency composition of texture-elicited vibrations

Next, we examined how the frequency composition of the vibrations changed with scanning speed. We found that, as anticipated, the power spectral density (PSD) shifted systematically towards higher frequencies as scanning speed increased (**Figure 3b**). However, the spectral structure of these vibrations was consistent across speeds when expressed in spatial units (by dividing the temporal frequency by the speed - **Figure 3c**). For surfaces with periodic structure, the shapes of these spatial power spectra closely matched the spatial power spectra of the surface microstructure, measured using a non-contact profilometer (**Figure 3d** and **Supplementary Figure 2**). In the case of aperiodic surfaces, whose physical surface spectra approximately fall at a rate of $^{1}/_{f}$ skin vibrations revealed a prominent component around 2 mm, which likely reflects the fingerprint's spatial period (7,11) (**Figure 3d**).

Having observed that the power of texture elicited vibrations varies across participants, we then assessed whether frequency composition also varied. To this end, we compared the normalized (40-600 Hz) PSDs (**Figure 2b**) and found significantly less variation within textures across participants (cross-validated Pearson's correlation, R2 = 0.741) than the converse (R2 = 0.469). Note that these comparisons disregard differences in overall power, which varies widely across participants as described above.

Speed-dependent changes in frequency drive changes in vibratory intensity

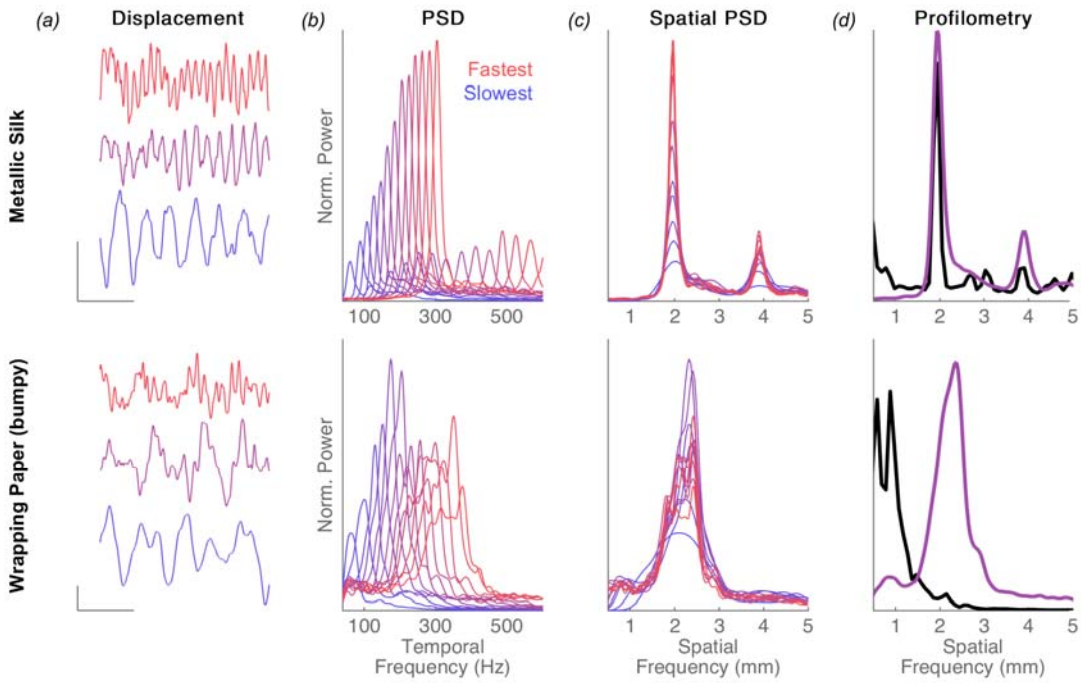

Figure 3 | Spectral characteristics of the vibrations are shifted in the temporal domain but conserved in the spatial domain. *(a)* Example displacement traces following presentation of either Metallic Silk (top) or Bumpy Paper (bottom) at 45, 100, and 150 mm/s. Scale bar is 25 ms and 50 µm. (*b*) Corresponding raw power spectral density shown in temporal and *(c)* spatial units for the adjacent traces and the intermediary speeds show the increase in temporal frequency but maintenance of spatial frequency with speed. *(d)* Profilometry for the same textures in spatial units shown that there is significant agreement between the vibrometry and profilometry periodicities for periodic textures (e.g. metallic silk) but not aperiodic (e.g. bumpy paper). See **Supplementary Figure 2** for temporal and spatial PSDs for all textures.

Next, we investigated whether the speed-dependent increase in energy results from the observed speed-dependent translation of the frequency composition of the vibrations. Accordingly, we warped the PSDs evoked by each texture at an intermediate speed (90 mm/s) to that expected at the target speed (Figure 4a). So, for example, the PSD at 45 mm/s would be the same as the vibration at 90 mm/s but shifted leftward in the frequency domain. If the only effect of speed is to dilate or contract the skin vibrations, then the resulting warped PSDs would match the measured ones (Figure 4b). We found that this simple model captured most of the structure in the measurements (Pearson's R2 = 0.83, normalized prediction error = 0.171, Figure 4c and **Supplementary Figure 3**). Furthermore, the predictions of this model were robust to changes in the choice of reference speed though there was a slight tendency for prediction error to decrease at higher reference speeds. In summary, using this warping approach, the vibrations elicited by a given texture at a given speed in a given participant can be used to predict the energy for that participant and texture at any speed.

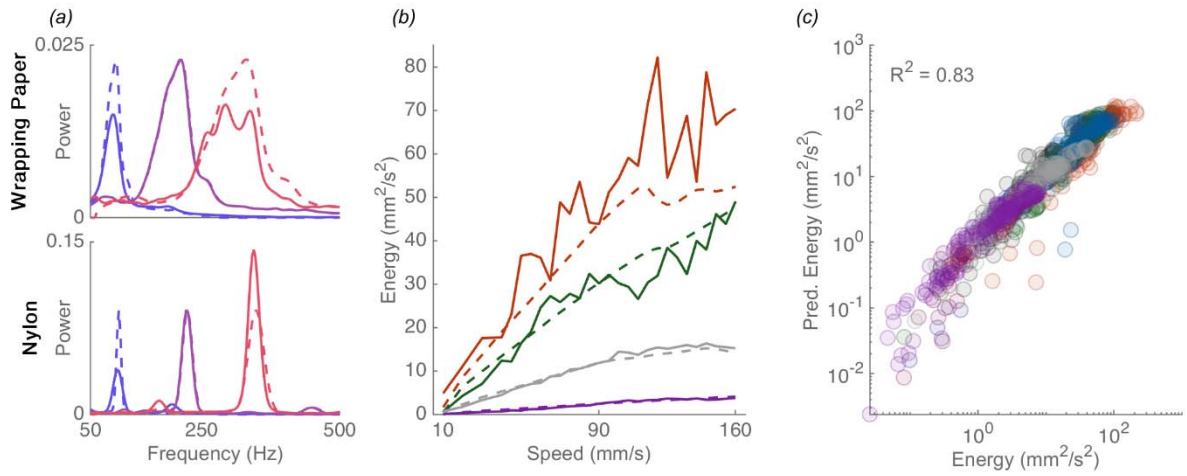

Figure 4 | Dilations or contractions of the vibrations accounts for the effect of speed on vibratory energy. *(a)* Solid lines show PSDs at 3 speeds (40, 90, and 140 mm/s) for two textures, dashed lines show the PSDs obtained by warping a trace obtained at 90 mm/s. At higher speeds, traces become wider and contribute more spectral power. *(b)* Recorded and predicted energy based on warping the 90 mm/s trace, predictions again displayed as dashed lines. (*c*) Measured energy versus predicted energy for every participant, texture, and speed - total n = 1091. See **Supplementary Figure 3** for predictions for individual participants and residuals for each texture. Color-scheme follows that of **Figure 2**.

DISCUSSION

Implications for texture perception

Texture perception is highly independent of scanning speed and contact force despite the fact that the response of the skin and that of tactile nerve fibers is highly dependent on these exploratory parameters (6,12). Indeed, the firing rates of tactile nerve fibers, particularly PC fibers, increase with increases in scanning speed. Here, we show that the effect of speed on afferent responses is mediated by an increase in vibratory power (3), itself caused by a translation of the frequency composition of the vibrations to higher frequencies. The enhancement of high frequency components of texture-evoked vibrations explains why the effect of speed is most pronounced in the responses of PC fibers, which are most sensitive at the high frequencies (> 100 Hz), weaker in RA fibers, which exhibit a preference for intermediate frequencies, and weakest for SA1 fibers, most sensitive at the lowest frequencies. While the peripheral representation of texture is highly speed dependent, afferent signals are differentiated downstream – spatially and temporally –, and these neural computations give rise to a more speed-independent representation of texture (13).

Implications to speed perception

While we have a sense of how fast a surface is moving across our skin (14,15), tactile speed perception is powerfully biased by surface texture: coarser textures are systematically perceived as moving faster. That speed perception is not veridical can be explained by its neural basis. Indeed, perceived speed is determined by the strength of the response evoked in PC fibers, itself dependent on both texture and scanning speed. In the present study, we replicate the finding that vibratory power is strongly dependent on surface texture. We also show that vibratory power is strongly dependent on speed.

Given that vibratory power at the high frequencies (> 50 Hz) is a good proxy for PC firing rates, the present results account for the dependence of perceived speed on both speed and texture (15).

Artificial textures

The rise of mobile devices – tablets and phones – has spurred the development of haptic interfaces to provide tactile feedback during manual interactions with the devices, most commonly in the form of vibrations triggered by contact with the screen. That texture perception relies on vibration has engendered attempts to produce textural percepts by generating texture-like vibrations on the surface (16–20). Because texture-elicited vibrations depend on both the texture and the exploratory parameters, a challenge in generating artificial textures has been to store the information necessary to replay vibrations appropriate for a given texture and a given set of exploratory parameters. One approach consists in tiling the space of possible scanning speeds and contact forces and interpolating between these measured values (20). Our results suggest that a more parsimonious approach would be to store the vibratory profile of each texture at some intermediate speed (say 90 mm/s) and warping said trace depending on the instantaneous scanning speed. The resulting vibrations would largely match their natural counterparts while relying on a single stored trace.

METHODS

Participants

Five subjects (2 men, 3 women, 20-25 years of age) participate in this study. Procedures were approved by the Institutional Review Board of the University of Chicago.

Data Collection

Texture apparatus and stimuli: The subject sat with the arm immobilized, palm facing upwards, and the index finger held at a 45-degree angle. On each trial, a rotating drum stimulator (previously described in Weber et al. 2013, shown in **Figure 1**) scanned one of eight texture strips (2.5 cm x 16 cm) across the subject's fingertip at a pre-calibrated contact force (30 g) and at one of 28 speeds, ranging from 10 to 160 mm/s, evenly spaced. Trial duration ranged from 0.4 seconds at the fastest speed to 1.6 seconds at the slowest one and the inter-trial duration was 3.5 s.

Vibrometer: A laser-doppler vibrometer (Polytec OFV-3001 with OFV 311 sensor head; Polytec, Irvine, CA) was used to record the vibrations elicited in the skin (cf. (7,21). Briefly, the vibrometer measures the time-varying velocity along the axis perpendicular to the surface of the skin, without making contact with it. Each subject's index finger was cleaned with an alcohol wipe and a small strip of white-out correction fluid (BIC USA, Shelton, CT, USA) was applied just distal of the distal interphalangeal joint of the right index finger – near the location where the finger made contact with the surface – to improve the reflectance of the finger and reduce drop outs. The vibrometer beam was then directed on the white out.

Profilometry: A laser confocal microscope (Olympus LEXT OLS5000, Tokyo, Japan) with a 10x dedicated objective was used to map an area 17.4 x 1.2 mm consisting of 15 areas (each 1.2 mm2) stitched along the scanning direction. The resolution of the height map was 1.25 µm along the x & y axes and 0.01 µm along the z axis. The heightmap was deplaned using linear regression and the power spectral density

(pwelch, Matlab 2018b, MathWorks, Natick, MA, USA) was computed for each column of pixels (the scanning direction) and the average taken.

Data Analysis

Preprocessing of vibrometry: Only the last 350 ms (35,000 data points) of each trace was used to exclude transients caused by the establishment of contact with the surface and ensure that the frequency resolution of the power spectra was equivalent across speeds. On each trace, outliers – which fell 6 SD from the mean for that speed/texture pair – were replaced by linear interpolation of the two adjacent time points. This process of outlier-removal was performed iteratively until all were removed. Traces that contained 2 ms or more of outliers were eliminated.

Spectral analysis: Power spectral densities were also computed using Welch's method. Frequencies were corrected for decay over 1 cm (see (21)) and the energy was computed over the range from 40 and 600 Hz unless otherwise stated. To convert the spectra to the spatial domain, each frequency was divided by the scanning speed (mm/s). To examine the cumulative displacement an FFT was performed, the frequency magnitudes were divided by $2\pi f$, and then an IFFT was subsequently performed to produce a displacement trace with the phases maintained.

Differences across textures and subjects: When analyzing the within subject versus within texture PSD analysis, we calculated the cross-validated Pearson's correlation coefficient. In the case of within subject variation, the PSD between 40 and 600 Hz of each texture was correlated with the mean of all remaining textures and the average value reported. For the within texture comparisons, we compared the PSD of each participant for a single texture against the mean PSD of all remaining participants for the same texture. For pairwise comparisons, we report the average of all comparisons.

Warping: To obtain the warped spectrum at speed S_{warp}, we first multiplied each frequency of the Fourier spectrum at S_{ref} by the ratio S_{warp}/S_{ref} then resampled the resulting spectrum such that the frequency resolution at S_{warp} matched that at S_{ref}.

Model evaluation: then quantify the quality of the predictions of the warping model, we used both Pearson's R2 and the range-normalized mean squared error, given by:

$$rnMSE = \frac{\sqrt{\sum(y - \hat{y})^2}}{y_{max} - y_{min}}$$

where y is the measured energy and $\hat{y}$ is the predicted energy.

Funding: This work was supported by National Institute of Health/National Institute of Neurological Disorders and Stroke grant RO1 NS 101325 and by NSF grant IIS-1518614 awarded to S.J.B.

Author contributions: S.J.B., C.M.G., and J.D.L. conceived of and designed the experiment. C.M.G. and K.R.M. collected the data. C.M.G. analyzed the data. C.M.G. and S.J.B. wrote the manuscript while J.D.L. provided critical feedback.

REFERENCES

1. Lederman SJ, Klatzky RL. Extracting object properties through haptic exploration. Acta Psychol (Amst) [Internet]. 1993 Oct;84(1):29–40. Available from: https://linkinghub.elsevier.com/retrieve/pii/0001691893900708

2. Hollins M, Risner SR. Evidence for the duplex theory of tactile texture perception. Percept Psychophys. 2000 May;62(4):695–705.

3. Bensmaia SJ, Hollins M. The vibrations of texture. Somatosens Mot Res. 2003;20(1).

4. Bensmaia SJ, Hollins M. Pacinian representations of fine surface texture. Percept Psychophys. 2005;67(5).

5. Hollins M, Bensmaia SJ, Washburn S. Vibrotactile adaptation impairs discrimination of fine, but not coarse, textures. Somatosens Mot Res. 2001;18(4).

6. Weber AI, Saal HP, Lieber JD, Cheng J-W, Manfredi LR, Dammann JF, et al. Spatial and temporal codes mediate the tactile perception of natural textures. PNAS [Internet]. 2013 Oct 15 [cited 2018 Dec 26];110(42):17107–12. Available from: http://www.ncbi.nlm.nih.gov/pubmed/24082087

7. Manfredi LR, Saal HP, Brown KJ, Zielinski MC, Dammann JF, Polashock VS, et al. Natural scenes in tactile texture. J Neurophysiol [Internet]. 2014 May [cited 2018 Oct 15];111(9):1792–802. Available from: http://www.ncbi.nlm.nih.gov/pubmed/24523522

8. Greenspan JD. Influence of velocity and direction of surface-parallel cutaneous stimuli on responses of mechanoreceptors in feline hairy skin. J Neurophysiol [Internet]. 1992 Sep [cited 2019 Apr 11];68(3):876–89. Available from: http://www.ncbi.nlm.nih.gov/pubmed/1432054

9. Dépeault A, Meftah E-M, Chapman CE. Neuronal correlates of tactile speed in primary somatosensory cortex. J Neurophysiol [Internet]. 2013 Oct [cited 2019 Mar 25];110(7):1554–66. Available from: http://www.ncbi.nlm.nih.gov/pubmed/23843433

10. Callier T, Saal HP, Davis-Berg EC, Bensmaia SJ. Kinematics of unconstrained tactile texture exploration. J Neurophysiol [Internet]. 2015 Apr 1 [cited 2018 Dec 26];113(7):3013–20. Available from: http://www.ncbi.nlm.nih.gov/pubmed/25744883

11. Scheibert J, Leurent S, Prevost A, Debrégeas G. The role of fingerprints in the coding of tactile information probed with a biomimetic sensor. Science (80-) [Internet]. 2009 Mar 13 [cited 2019 Apr 23];323(5920):1503–6. Available from: http://www.ncbi.nlm.nih.gov/pubmed/19179493

12. Saal HP, Suresh AK, Solorzano LE, Weber AI, Bensmaia SJ. The Effect of Contact Force on the Responses of Tactile Nerve Fibers to Scanned Textures. Neuroscience [Internet]. 2018 Oct 1 [cited 2018 Dec 26];389:99–103. Available from: https://www.sciencedirect.com/science/article/pii/S0306452217305900#b0130

13. Lieber JD, Bensmaia SJ. Emergence of an invariant representation of texture in primate somatosensory cortex. bioRxiv [Internet]. 2019 May 24 [cited 2019 Jun 24];646042. Available from: https://www.biorxiv.org/content/10.1101/646042v1

14. Dépeault A, Meftah E-M, Chapman CE. Tactile Speed Scaling: Contributions of Time and Space. J Neurophysiol [Internet]. 2008 Mar [cited 2019 May 9];99(3):1422–34. Available from:

http://www.physiology.org/doi/10.1152/jn.01209.2007

15. Delhaye BP, O'Donnell MK, Lieber JD, McLellan KR, Bensmaia SJ. FEELING FOOLED: TEXTURE CONTAMINATES THE NEURAL CODE FOR TACTILE SPEED. PLOS Biol. 2019;

16. Shultz C, Peshkin M, Colgate JE. The Application of Tactile, Audible, and Ultrasonic Forces to Human Fingertips Using Broadband Electroadhesion. IEEE Trans Haptics [Internet]. 2018 Apr 1 [cited 2019 May 9];11(2):279–90. Available from: https://ieeexplore.ieee.org/document/8259336/

17. Kuchenbecker KJ, Fiene J, Niemeyer G. Improving contact realism through event-based haptic feedback. IEEE Trans Vis Comput Graph [Internet]. 2006 Mar [cited 2019 May 9];12(2):219–30. Available from: http://ieeexplore.ieee.org/document/1580456/

18. Choi S, Kuchenbecker KJ. Vibrotactile Display: Perception, Technology, and Applications. Proc IEEE [Internet]. 2013 Sep [cited 2019 May 9];101(9):2093–104. Available from: http://ieeexplore.ieee.org/document/6353870/

19. Altinsoy ME, Merchel S. Electrotactile Feedback for Handheld Devices with Touch Screen and Simulation of Roughness. IEEE Trans Haptics [Internet]. 2012 Jan [cited 2019 May 9];5(1):6–13. Available from: http://ieeexplore.ieee.org/document/6042861/

20. Culbertson H, Unwin J, Kuchenbecker KJ. Modeling and Rendering Realistic Textures from Unconstrained Tool-Surface Interactions. IEEE Trans Haptics [Internet]. 2014 Jul 1 [cited 2019 Jun 5];7(3):381–93. Available from: http://ieeexplore.ieee.org/document/6787087/

21. Manfredi LR, Baker AT, Elias DO, Dammann JF, Zielinski MC, Polashock VS, et al. The Effect of Surface Wave Propagation on Neural Responses to Vibration in Primate Glabrous Skin. Maravall M, editor. PLoS One [Internet]. 2012 Feb 13 [cited 2018 Oct 15];7(2):e31203. Available from: http://www.ncbi.nlm.nih.gov/pubmed/22348055

SUPPLEMENTARY FIGURES

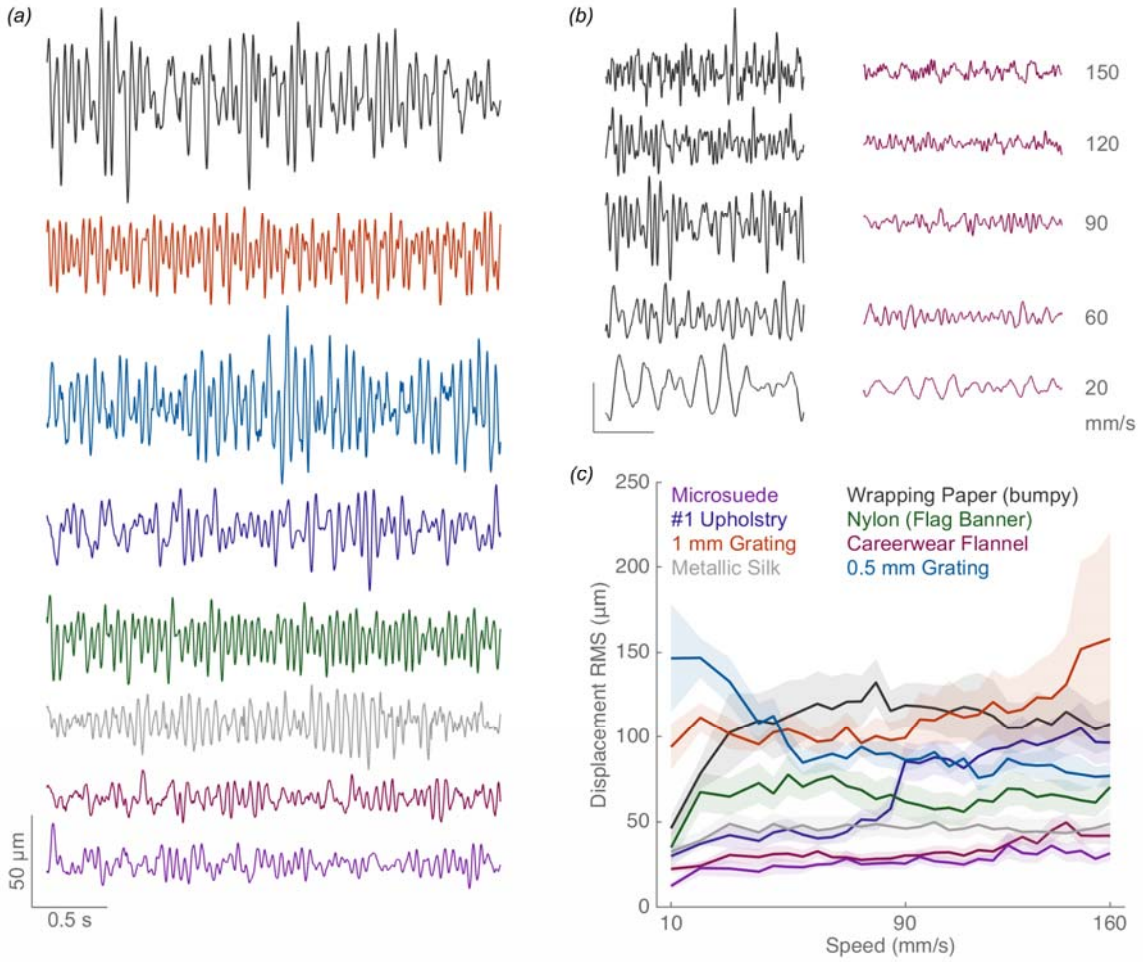

Supplementary Figure 1 | Skin displacement over time. *(a)* Example displacement traces for each texture (legend shown in *panel c*) scanned over the skin at 90 mm/s. *(b)* Vibrations elicited when wrapping paper and flannel are scanned across the skin at several speeds. *(c)* RMS amplitude averaged across subjects vs. speed for the 8 textures.

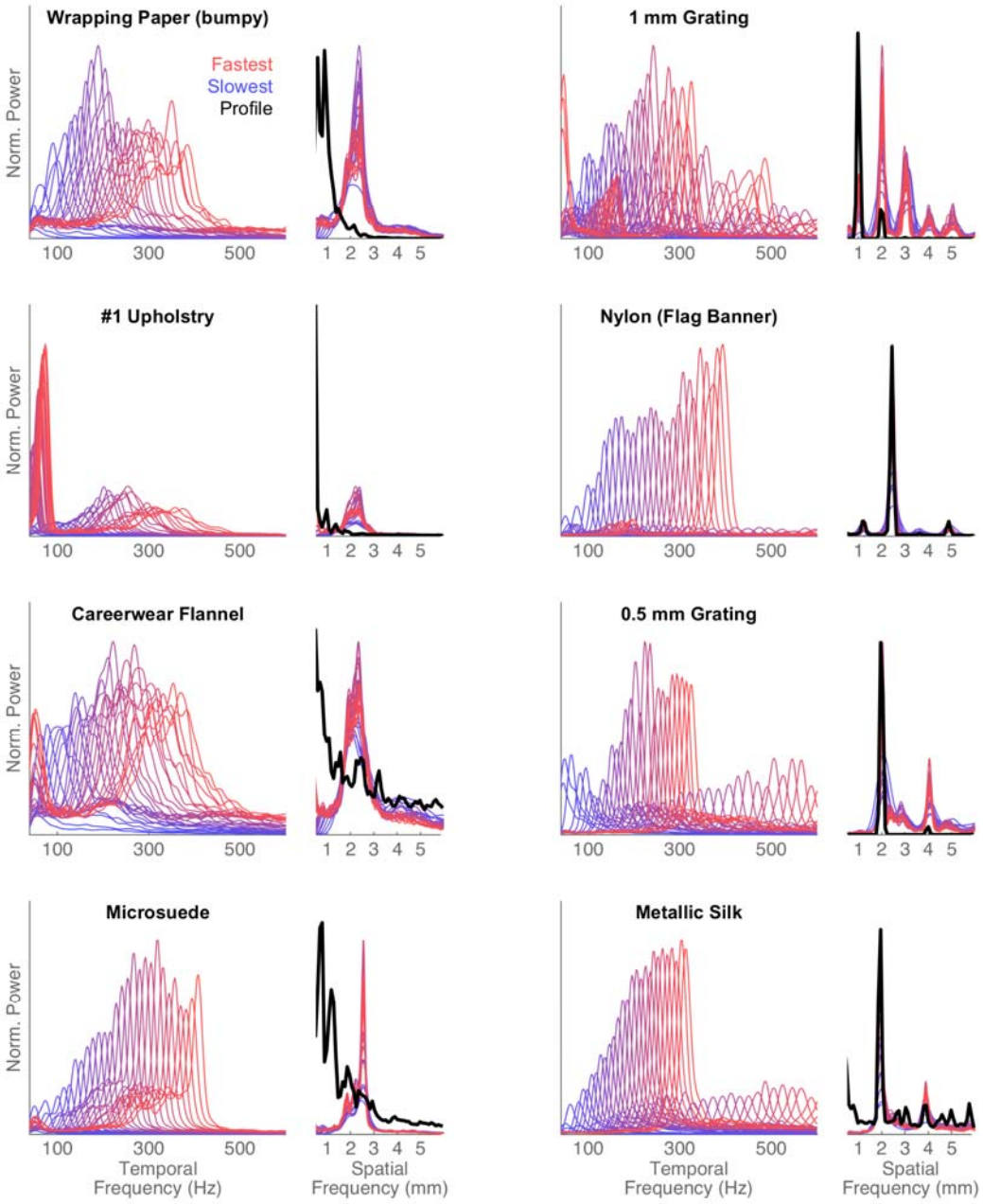

Supplementary Figure 2 | Normalized power spectra for all textures at all speeds. Power spectra in the temporal (left) and spatial (right) domains for aperiodic (right) and period (left) textures. Increases in speed result in rightward shifts in temporal frequency but not in spatial frequency.

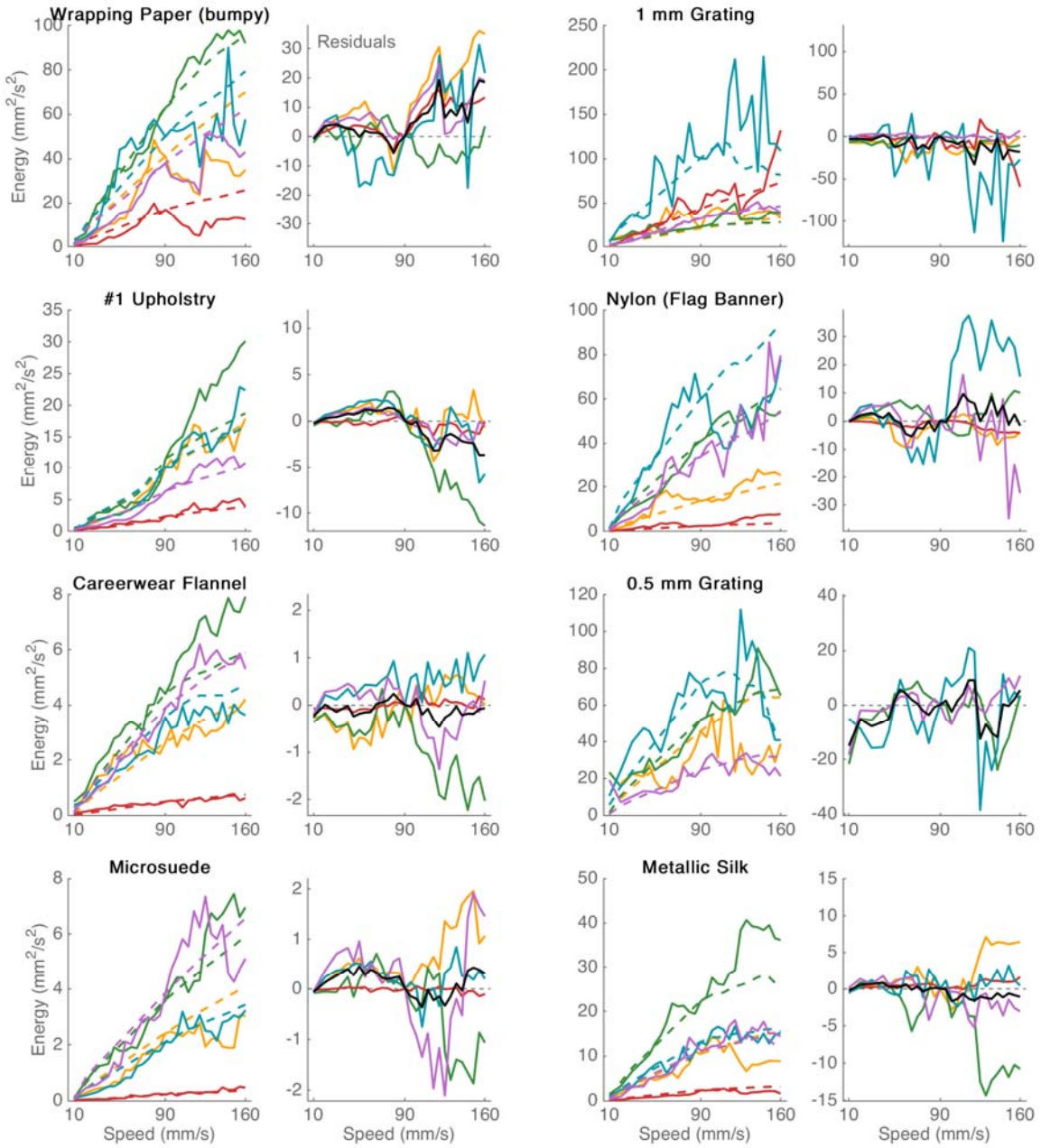

Supplementary Figure 3 | Energy predictions based on warping the 90 mm/s trace for each texture and participant (shown in individual colors). Predictions are shown in dashed lines. Residuals for each participant are shown to the right and the mean residual in black. The model accurately accounts for variations across both textures and participants (each represented by a different color).